

This is a repository copy of *Magneto-optic probe measurements in low density-supersonic jets*.

White Rose Research Online URL for this paper:

<https://eprints.whiterose.ac.uk/126101/>

Version: Accepted Version

Article:

Oliver, David M, White, T. G., Maybe, P. et al. (21 more authors) (2017) Magneto-optic probe measurements in low density-supersonic jets. *Journal of Instrumentation*. P12001. ISSN 1748-0221

<https://doi.org/10.1088/1748-0221/12/12/P12001>

Reuse

Items deposited in White Rose Research Online are protected by copyright, with all rights reserved unless indicated otherwise. They may be downloaded and/or printed for private study, or other acts as permitted by national copyright laws. The publisher or other rights holders may allow further reproduction and re-use of the full text version. This is indicated by the licence information on the White Rose Research Online record for the item.

Takedown

If you consider content in White Rose Research Online to be in breach of UK law, please notify us by emailing eprints@whiterose.ac.uk including the URL of the record and the reason for the withdrawal request.

Magneto-optic probe measurements in low density-supersonic jets

M. T. Oliver,¹ T. G. White,¹ P. Mabey,¹ M. Kühn-Kauffeldt,² L. Döhl,³ R. Bingham,^{4,5}
R. Clarke,⁴ P. Graham,⁶ R. Heathcote,⁴ M. Koenig,⁷ Y. Kuramitsu,⁸ D. Q. Lamb,⁹ J.
Meinecke,¹ T. Michel,⁷ F. Miniati,¹⁰ M. Notley,⁴ B. Reville,¹¹ S. Sarkar,¹ Y. Sakawa,¹²
A. A. Schekochihin,¹ P. Tzeferacos,⁹ N. Woolsey,¹³ and G. Gregori¹

¹*Department of Physics, University of Oxford, Parks Road, Oxford OX1 3PU,
UK*

²*Universität der Bundeswehr München, Neubiberg, Germany*

³*Department of Physics University of York, Heslington, York, YO10 5DD,
UK*

⁴*Rutherford Appleton Laboratory, Chilton, Didcot OX11 0QX,
UK*

⁵*Department of Physics, University of Strathclyde, Glasgow G4 0NG,
UK*

⁶*AWE, Aldermaston, Reading, West Berkshire, RG7 4PR,
UK*

⁷*Laboratoire pour l'Utilisation de Lasers Intenses, UMR7605, CNRS CEA,
Université Paris VI Ecole Polytechnique, 91128 Palaiseau Cedex,
France*

⁸*National Central University, Taoyuan, Taiwan*

⁹*Department of Astronomy and Astrophysics, University of Chicago,
5640 S. Ellis Ave, Chicago, IL 60637, USA*

¹⁰*ETH Zurich, Zurich, Switzerland*

¹¹*School of Mathematics and Physics, Queens University Belfast, Belfast BT7 1NN,
UK*

¹²*Institute of Laser Engineering, Osaka, Japan*

¹³*Department of Physics University of York, Heslington, York, YO10 5DD,
UK*

(Dated: 1 June 2017)

A magneto-optic probe was used to make time-resolved measurements of the magnetic field in both a single supersonic jet and in a collision between two supersonic turbulent jets, with an electron density $\approx 10^{18} \text{ cm}^{-3}$ and electron temperature $\approx 4 \text{ eV}$. The magneto-optic data indicated the magnetic field reaches $B \approx 200 \text{ G}$. The measured values are compared against those obtained with a magnetic induction probe. Good agreement of the time-dependent magnetic field measured using the two techniques is found.

I. INTRODUCTION

Magnetic fields play an important role in plasma dynamics and particle acceleration in astrophysics^{1–6}. This has led, in the past decade, to a wide range of laboratory experiments aimed at examining the amplification, structure, and dissipation of these fields^{7–12}. Clearly, the understanding of the property of the magnetic fields in plasma require accurate diagnostics. The magnetic induction (B-dot) probe is a practical, accurate and sensitive instrument, able to make well-resolved field measurements¹³. However, this comes with several drawbacks. First of all, the B-dot is a mechanical probe that must be inserted into the plasma. This inevitably perturbs the properties of the plasma. To compensate for this, the probe must be miniaturized, such that its linear dimensions are smaller than the relevant spatial scales of interest. This poses several constraints on its construction, as a suitable B-dot probe for use in laboratory astrophysics experiments requires a bandwidth which is fast enough to resolve the dynamics of the flow¹³.

Because of this, optical diagnostics may be advantageous. While the Zeeman effect, for example, offers an entirely non-invasive method of measuring the field, the spectral line splitting for typical plasma conditions in these experiments is of the order of other line broadening mechanisms, such as Doppler or Stark broadening^{14,15}. Considering an emission line with wavelength $\lambda = 400$ nm, a $B = 200$ G field gives an induced broadening due to Zeeman $\frac{\Delta\lambda}{\lambda} \sim 10^{-4}$, far smaller than the Doppler broadening at electronvolt temperatures. Faraday rotation of a probe laser is another commonly used technique for the measurements of magnetic fields¹⁶. However, for optical wavelengths, this requires the product of the magnetic field and plasma density to be large enough, typically requiring electron plasma densities $n_e \gtrsim 10^{18} \text{ cm}^{-3}$ for an appreciable rotation. For instance in a 1 cm long plasma with a uniform electron density of $n_e = 10^{18} \text{ cm}^{-3}$ and a uniform magnetic field $B = 200$ G, as in the experiment discussed in this paper, the change in the polarization rotation angle for a 532 nm probe beam would be less than 0.001° ¹⁶, which is challenging to measure. Alternatively, the Hanle effect, due to the depolarization of scattered light in atomic transitions involving magnetic sublevels, may also be used to measure fields in turbulent plasma. This has been applied to diagnose magnetic field in the solar atmosphere¹⁷. The Hanle effect has the advantage that, while the Faraday rotation cancels out on average in a turbulent magnetic field, the depolarization does not. However, when considering laboratory plasma conditions,

for $n_e \sim 10^{18} \text{ cm}^{-3}$, it produces a measurable signal only for fields $B > 1 \text{ kG}$ ¹⁸.

In presence of smaller magnetic fields, Faraday rotation measurements are still possible, but they require the use of a small birefringent crystal placed within the plasma to increase the rotation. Magneto-optical probes, relying on this enhancement of the Faraday rotation, have been tested with large current-driven magnetic fields^{19–21}. However, to our knowledge, they have not yet been used to measure smaller fluctuating magnetic fields in plasmas, nor tested against other diagnostics methods. Here, we discuss the results of an experiment aimed at measuring the magnetic field in a turbulent plasma. We compare the results from a magneto-optic probe to the measurements obtained with a B-dot probe.

As for the usual Faraday rotation, the magnitude of the rotation inside the birefringent crystal depends on the line integral of the component of the magnetic field along the laser path. As the electron density is constant in the crystal, the rotation angle, Φ , of an electromagnetic wave traveling along the axis of the crystal is given by

$$\Delta\Phi = V \int B(l)dl, \quad (1)$$

where V is known as the Verdet constant, $B(l)$ is longitudinal component of the magnetic field, and l is the length of the crystal. We used a terbium gallium garnet (TGG) crystal²², which has $V = 190 \text{ rad/T} \cdot \text{m}$ at $\lambda = 532 \text{ nm}$, the wavelength of probe laser used in our experiment. The average field along the length of the crystal (L) is therefore

$$\langle B \rangle = \Delta\Phi/VL. \quad (2)$$

The probe beam was linearly polarized before entering the crystal and split by a 50/50 beam-splitter after passing through the crystal. The polarization of light after the crystal is given simply by

$$\Phi = \arctan \sqrt{\frac{TI_s}{I_p}}, \quad (3)$$

where I_s and I_p are the intensities of the two orthogonal polarizations, and T is a factor accounting for different losses in each polarization due to losses in the optical pass and varying detector response. The factor T is found by setting $TI_s = I_p$ when no magnetic field is present.

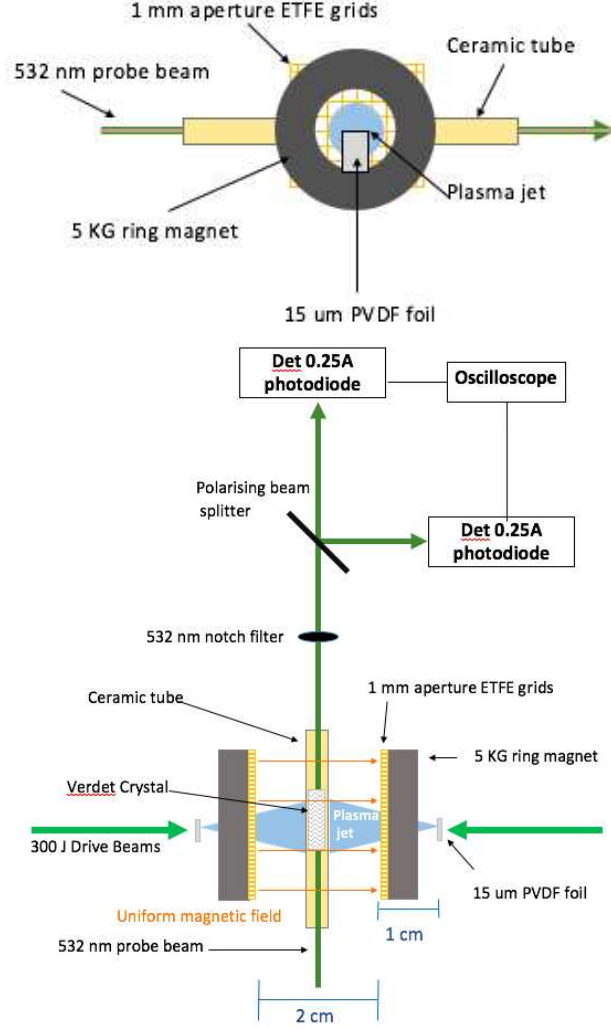


FIG. 1. (a) View of the target from the direction of incoming drive beam. The target is ablated creating a plasma jet which advects the field of the ring magnet and becomes turbulent as it passes through the grid. (b) Top-down view of target and magneto-optic probe setup. Once the jets have passed through the grid they collide with each other around the probe. The probe beam passes through the verdet crystal in the center of the two jets before entering the detection system.

II. EXPERIMENTAL SETUP

Both the Verdet crystal and B-dot probes were used as part of an experiment on supersonic turbulence performed at the Rutherford Appleton Laboratory (UK). The experimental setup is shown in Figure 1. The experiment consisted in creating two counter-propagating supersonic jets. Each jet was produced by firing three 2 ns long, ≈ 100 J, 527 nm 200 μm diameter focal spot drive beams onto a 10 μm thick fluorinated plastic (PVDF) target inside

of a vacuum chamber at an ambient pressure of $\approx 10^{-5}$ mbar. The jet passed through the central hole of a 5 kG ring magnet with a field parallel to the direction of the flow. The field was advected with the flow, which in the case of the turbulent jet then passed through a 1 mm aperture, 0.5 mm thick plastic (ETFE) grid, making the jet turbulent. The magnetic field measurements have been performed in the center of the interaction region, where the jets collide.

The Verdet crystal was held in the center of the colliding jets using an open-ended ceramic tube (outer diameter 2.5 mm, inner diameter 1.3 mm), with the axis of the crystal perpendicular to the incoming jets. The crystal had a diameter of 1 mm and a length of 10 mm. The purpose of the ceramic tube was to protect the Verdet crystal from hard radiation capable of reducing the opacity of the crystal and direct exposure to the plasma flow, as thermal heating can change its birefringence properties²³. Indeed, we estimate the time taken for heat from the plasma to diffuse through the ceramic tube to be approximately 10 μ s, much longer than the duration of the experiment. The probe laser had a wavelength of 532 nm (different from that of the drive beams on the PVDF foils) and was focused with a 1 mm lens to a focal spot of ≈ 0.5 μ m. The polarization of the probe beam was rotated using a half-wave plate to ensure it was at 45° to the optical axis of the beam-splitter before it passed through the crystal.

A optical line filter with a FWHM ≈ 1 nm was used to block any stray light from the target before the probe beam was divided by a 50/50 polarizing beam splitter; each polarization was then detected separately by a 2 GHz (DET0.25A Thorlabs) photo-diode connected to a 1 GHz Lecroy oscilloscope.

For comparison the magneto-optic probe was removed and replaced by the induction coil. The B-dot probe is a single axis probe with a single-turn coil with an effective area of 0.29 mm² protected by a 2.5 mm diameter glass tube. The coil was oriented such as to measure a symmetrically equivalent component of the magnetic field, that is the component of the magnetic field perpendicular to the bulk flow direction. The design and calibration of the probe has been described by Everson¹³. Calibration of the B-dot with a network analyzer determined the frequency resolution of probe to be 40 MHz. The B-dot probe was connected to the same 1 GHz oscilloscope as used in the Verdet setup.

The jet velocity is found using Schlieren imaging, the electron density from optical interferometry and the electron temperature is determined from emission spectroscopy. These

will be briefly discussed below.

III. RESULTS

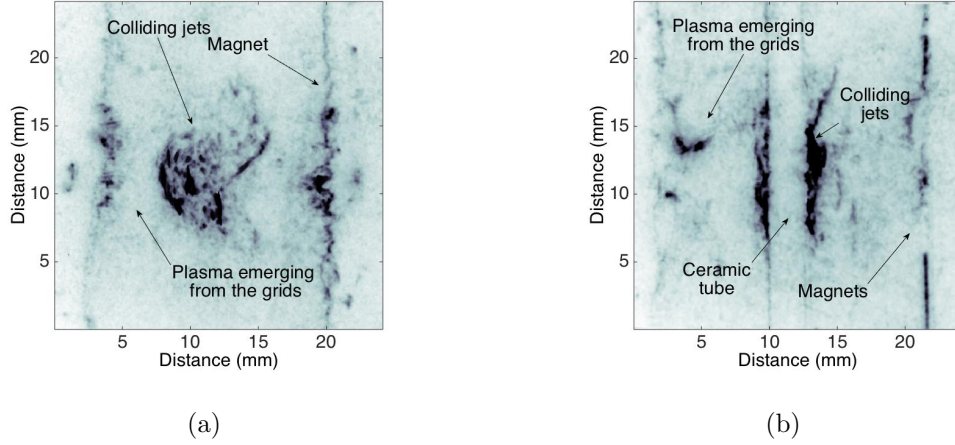
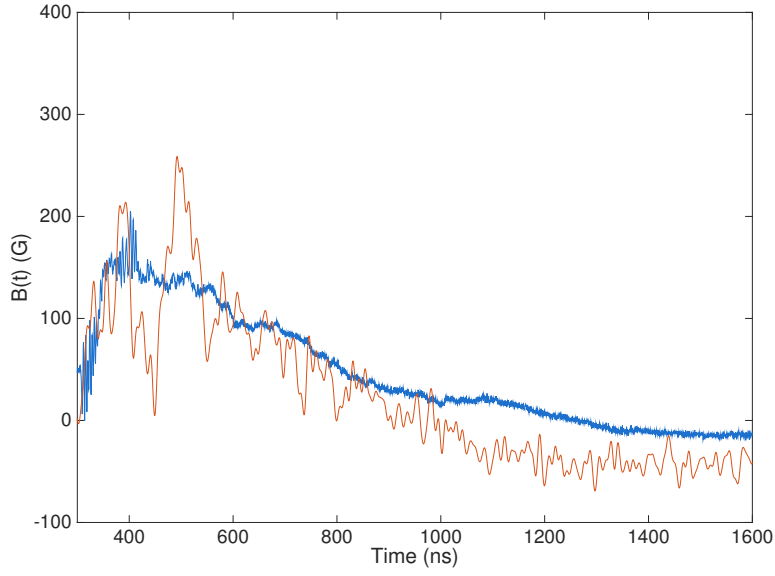


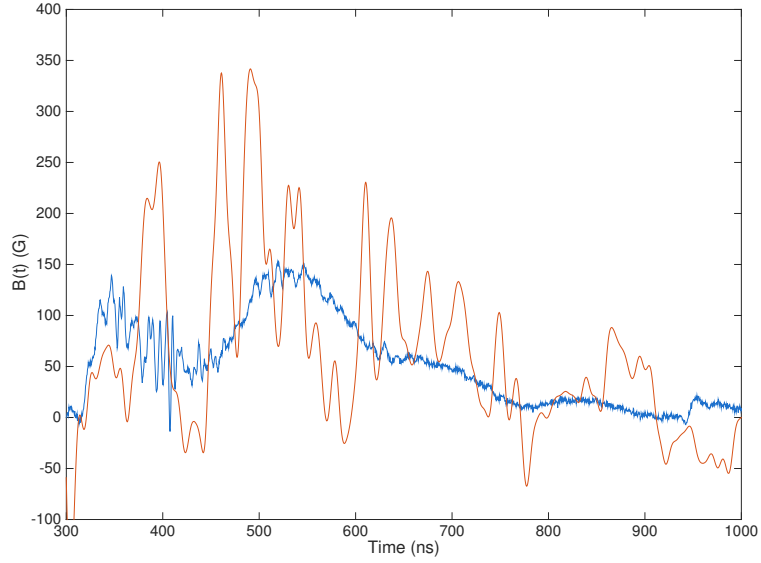
FIG. 2. Schlieren images of the collision area. The magnets can be seen at the sides of the image. Plasma is seen emerging from the grids, bordering the magnets. The collision of the two turbulent jets appears in the center of the image ($n_e \approx 10^{18} \text{ cm}^{-3}$). a) The turbulent plasma 700 ns after the collision (no Verdet probe present). b) The turbulent plasma around the Verdet probe 1000 ns after the collision.

Figure 2 shows Schlieren images of the colliding turbulent jets at 700 ns and 1000 ns after the drive beams have fired. The collision of the jets can be seen in the center of the image. At the sides the plasma can be seen emerging from the grids. In figure 2b we also see the outline of the ceramic tube enclosing the magneto-optic probe. From the schlieren image we find the turbulent plasma region has a volume of $\approx 1 \text{ cm}^{-3}$. The electron density is $\approx 10^{18} \text{ cm}^{-3}$ and the electron temperature is $\approx 4 \text{ eV}$ during the collision. It is clear from the images that the plasma is turbulent and remains around the probe for at approximately 600 ns after the collision.

Figure 3 shows the measured magnetic field intensity over the course of the experiment for both a single jet (a) and the collision of two turbulent jets (b). In both cases the field measured by the Verdet and the B-dot probes is similar, although the Verdet measurement shows larger-amplitude oscillations than the B-dot probe, particularly between 300 and 900



(a)



(b)

FIG. 3. The blue line shows the magnetic field measured by the B-dot probe and the orange line shows the magnetic field measured by the magneto-optic probe. a) A measurement taken for a single jet that has not passed through a grid. b) A measurement taken for two colliding, turbulent jets as the plasma collides and stagnates around the probe.

ns. Peak values of the magnetic fields are similar $B \approx 200\text{--}300$ G. However, it should be

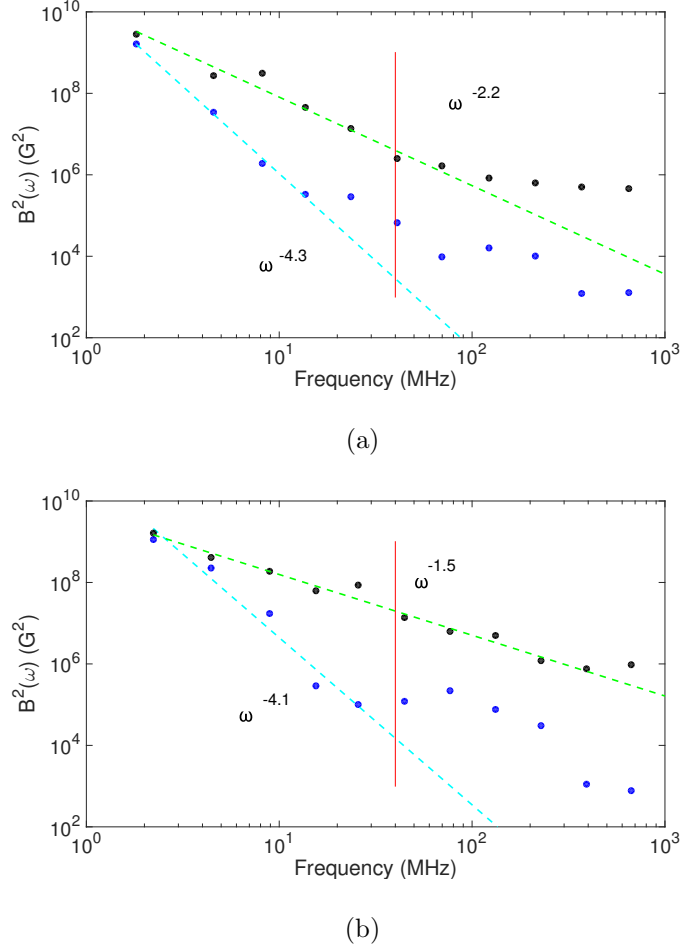


FIG. 4. The magnetic power spectra as a function of the frequency for both the B-dot (black markers) and magneto-optic (blue markers) probes. Straight lines are plotted to the linear parts of all the spectra. The red line shows the bandwidth of the B-dot probe. a) Spectra for a single jet. b) Spectra for the collision of two turbulent jets.

pointed out that the magnetic field measured by the Verdet crystal is averaged over the length of the crystal (see introduction), while in the case of the B-dot the field measurement occurs locally in the collision center. Whilst intuitively it would appear that the time-varying magnetic field should be smoother for a measurement integrated along a line of sight (i.e. the Verdet probe) than for the corresponding measurement made at a single point, this is not seen in the data. It is clear from the Schlieren data (see Figure 2) that for both a single jet and a turbulent plasma the spatial structure of the plasma density varies significantly over the length of the crystal. As the field from the permanent magnets is at least partly advected along with the plasma flow, an anisotropic density distribution suggests

there will also be a inhomogeneous magnetic field. The difference between the two probe measurements are likely due to the inhomogeneity and anisotropy of the plasma. Figure 4 shows the magnetic power spectra, $|B(\omega)|^2$ against $\omega/2\pi$ for the fields shown in figure 3. The bandwidth of the B-dot probe, ~ 40 MHz, is highlighted in the figure. The time resolution of the magneto-optic probe in the experiment is limited by the (low) intensity of the probe laser light reaching the photo-diodes, primarily due to the difficulty in focusing through the 1 mm diameter crystal. The bandwidth of the magneto-optical probe was determined to be ~ 100 MHz, comparable to the B-dot. Indeed, in Figure 4 we notice that the signal flattens between 60–100 MHz, indicating the start of the noise floor. A power law has been fitted to the linear part of the spectra, giving $\omega^{-4.3}$ – $\omega^{-4.1}$ for the B-dot case, and $\omega^{-2.2}$ – $\omega^{-1.5}$ for the Verdet measurement.

In order to explain these differences, let us assume that, at any given time t , the magnetic field at a point ℓ_0 is related to the magnetic field at a point ℓ along the axis of the TGG crystal by a relation

$$B(t, \ell) \sim B(t, \ell_0) \ell^p, \quad (4)$$

where ℓ_0 can be assumed to be the center of the Verdet crystal, where the B-dot measurement is taken, and p is a constant to be determined. From equations (2-4), we obtain

$$\langle B(t) \rangle \sim B(t, \ell_0) \ell^{p+1}. \quad (5)$$

Now, the power spectrum of the magnetic field measured at position ℓ_0 (as obtained from the B-dot data) is

$$M_0(\omega) \omega \sim |B(t, \ell_0)|^2 \sim \omega^{-\alpha+1}, \quad (6)$$

with $\alpha = 4.1$ – 4.3 . The power spectrum of the magnetic field integrated along ℓ (as obtained from the Magneto-optic probe data) is

$$M(\omega) \omega \sim \langle B(t) \rangle^2 \sim |B(t, \ell_0)|^2 \ell^{2(p+1)} \sim \omega^{-\beta+1}. \quad (7)$$

As the mean flow velocity in the plasma is larger than the velocity fluctuations, then, according to Taylors hypothesis, $\ell \sim t$. As a result of this proportionality relation, $\beta = \alpha + 2(p + 1)$. Since the measurement gives $\beta = 1.5$ – 2.2 , we deduce that $p \sim -2$. That is, the magnetic field has a real space distribution as

$$B(t, \ell) \approx \frac{B(t, \ell_0)}{\ell^2}, \quad (8)$$

indicating that the magnetic field rapidly decays away from the central region. This shows that the combination of Verdet and B-dot measurements can retrieve important information on both the temporal and spatial structure of the magnetic field.

IV. SUMMARY

A probe based on optical Faraday rotation has been used to measure the time-dependent magnetic field in a jet and in a collision between turbulent jets. In both cases the measured fields and spectra were compared to measurements taken by a magnetic induction probe. We show that the two measurements yield identical results if the magnetic field is assumed to rapidly decay away from the center of the interaction region. The principle benefit of a magneto-optic probe over the magnetic induction probe is its improved bandwidth, as is demonstrated in figure 4.

V. ACKNOWLEDGEMENTS

This work was supported by the Engineering and Physical Sciences Research Council (grant numbers EP/M022331/1 and EP/N014472/1), the Science and Technology Facilities Council of the United Kingdom, and by AWE plc.

REFERENCES

- ¹A. A. Schekochihin and S. C. Cowley, *Physics of Plasmas* **13** (2006), 10.1063/1.2179053, arXiv:0601246 [astro-ph].
- ²D. Ryu, H. Kang, J. Cho, and S. Das, *Science* **320**, 909 (2008), arXiv:0805.2466.
- ³E. G. Zweibel and C. Heiles, “Magnetic fields in galaxies and beyond,” (1997).
- ⁴A. Marcowith, A. Bret, A. Bykov, M. E. Dieckman, L. O. Drury, B. Lembège, M. Lemoine, G. Morlino, G. Murphy, G. Pelletier, I. Plotnikov, B. Reville, M. Riquelme, L. Sironi, and A. S. Novo, *Reports on progress in physics. Physical Society (Great Britain)* **79**, 046901 (2016), arXiv:1604.00318.
- ⁵R. J. van Weeren, H. J. A. Röttgering, M. Brüggen, and M. Hoeft, *Science* **330**, 347 (2010), arXiv:1010.4306.
- ⁶R. Blandford and D. Eichler, *Physics Reports* **154**, 1 (1987).

- ⁷N. L. Kugland, D. D. Ryutov, P.-Y. Chang, R. P. Drake, G. Fiksel, D. H. Froula, S. H. Glenzer, G. Gregori, M. Grosskopf, M. Koenig, Y. Kuramitsu, C. Kuranz, M. C. Levy, E. Liang, J. Meinecke, F. Miniati, T. Morita, A. Pelka, C. Plechaty, R. Presura, A. Ravasio, B. A. Remington, B. Reville, J. S. Ross, Y. Sakawa, A. Spitkovsky, H. Takabe, and H.-S. Park, *Nature Physics* **8**, 809 (2012).
- ⁸H. S. Park, C. M. Huntington, F. Fiuza, R. P. Drake, D. H. Froula, G. Gregori, M. Koenig, N. L. Kugland, C. C. Kuranz, D. Q. Lamb, M. C. Levy, C. K. Li, J. Meinecke, T. Morita, R. D. Petrasso, B. B. Pollock, B. A. Remington, H. G. Rinderknecht, M. Rosenberg, J. S. Ross, D. D. Ryutov, Y. Sakawa, A. Spitkovsky, H. Takabe, D. P. Turnbull, P. Tzeferacos, S. V. Weber, and A. B. Zylstra, *Physics of Plasmas* **22** (2015), 10.1063/1.4920959.
- ⁹G. Gregori, A. Ravasio, C. D. Murphy, K. Schaar, A. Baird, A. R. Bell, A. Benuzzi-Mounaix, R. Bingham, C. Constantin, R. P. Drake, M. Edwards, E. T. Everson, C. D. Gregory, Y. Kuramitsu, W. Lau, J. Mithen, C. Niemann, H.-S. Park, B. A. Remington, B. Reville, A. P. L. Robinson, D. D. Ryutov, Y. Sakawa, S. Yang, N. C. Woolsey, M. Koenig, and F. Miniati, *Nature* **481**, 480 (2012).
- ¹⁰J. Meinecke, H. Doyle, F. Miniati, and A. Bell, *Nature Physics* **10**, 2 (2014).
- ¹¹J. Meinecke, P. Tzeferacos, A. Bell, R. Bingham, R. Clarke, E. Churazov, R. Crowston, H. Doyle, R. P. Drake, R. Heathcote, M. Koenig, Y. Kuramitsu, C. Kuranz, D. Lee, M. MacDonald, C. Murphy, M. Notley, H.-S. Park, A. Pelka, A. Ravasio, B. Reville, Y. Sakawa, W. Wan, N. Woolsey, R. Yurchak, F. Miniati, A. Schekochihin, D. Lamb, and G. Gregori, *Proceedings of the National Academy of Sciences* **112**, 8211 (2015), arXiv:arXiv:1408.1149.
- ¹²C. Niemann, W. Gekelman, C.G. Constantin, E. T. Everson, D. B. Schaeffer, A. S. Bondarenko, S. E. Clark, D. Winske, S. Vincena, B. Van Compernelle, and P. Pribyl, *Geophysical Research Letters* **41**, 7413 (2014).
- ¹³E. T. Everson, P. Pribyl, C. G. Constantin, A. Zylstra, D. Schaeffer, N. L. Kugland, and C. Niemann, *Review of Scientific Instruments* **80**, 1 (2009).
- ¹⁴F. C. Jahoda, F. L. Ribe, and G. A. Sawyer, *Physical Review* **131**, 24 (1963).
- ¹⁵E. a. McLean, J. a. Stamper, C. K. Manka, H. R. Griem, D. W. Droemer, and B. H. Ripin, *Physics of Fluids* **27**, 1327 (1984).
- ¹⁶I. H. Hutchinson, *Plasma Physics and Controlled Fusion* **44**, 2603 (2002), arXiv:arXiv:1011.1669v3.

- ¹⁷J. O. Stenflo, *Solar Physics* **80**, 209 (1982).
- ¹⁸R. Presura, *Review of Scientific Instruments* **83** (2012), 10.1063/1.4739233.
- ¹⁹S. E. Clark, D. B. Schaeffer, A. S. Bondarenko, E. T. Everson, C. G. Constantin, and C. Niemann, *Review of Scientific Instruments* **83**, 1 (2012).
- ²⁰W. S. Przybysz, J. Ellis, S. C. Thakur, A. Hansen, R. A. Hardin, S. Sears, and E. E. Scime, *Review of Scientific Instruments* **80**, 1 (2009).
- ²¹S. Fujioka, Z. Zhang, K. Ishihara, K. Shigemori, Y. Hironaka, T. Johzaki, A. Sunahara, N. Yamamoto, H. Nakashima, T. Watanabe, H. Shiraga, H. Nishimura, and H. Azechi, *Scientific reports* **3**, 1170 (2013).
- ²²A. B. Villaverde, D. A. Donatti, and D. G. Bozinis, *Journal of Physics C: Solid State Physics* **11**, L495 (2001).
- ²³N. P. Barnes and L. B. Petway, “Variation of the Verdet constant with temperature of terbium gallium garnet,” (1992).